Innovative Infrastructure Solutions (2026) 11:155
https://doi.org/10.1007/s41062-026-02564-7

STATE-OF-THE-ART PAPER

Impact of moderate and high-temperature cyclic heating on lateritic soil properties

Olubunmi Oluwadare Owoyemi[1] · Lekan Olatayo Afolagboye[2] · Megan Welman-Purchase[3] · Charles Adebayo Oyelami[4]

Received: 18 June 2024 / Accepted: 13 February 2026
© Springer Nature Switzerland AG 2026

Abstract

This study examines the effects of cyclic moderate and high-temperature heating on the mineralogical, microstructural, and geotechnical properties of lateritic soils. Residual soils from Akerebiata (AK) and Ipetu (IP), southwestern Nigeria, were subjected to five heating–cooling cycles at 300 °C and 500 °C, using a heating rate of 5 °C/min. Mineralogical and microstructural changes were evaluated using X-ray diffraction (XRD) and scanning electron microscopy (SEM), while geotechnical properties were assessed using standard laboratory tests and supported by one-way and two-way ANOVA with Tukey's HSD post-hoc analysis. Cyclic heating caused significant mineralogical alteration in the feldspar-rich AK soil, marked by a reduction in plagioclase and an increase in quartz content. In contrast the kaolinite quartz dominated IP soil remained largely mineralogically stable. SEM observations revealed progressive particle agglomeration in both soils and particularly more pronounced at 500 °C. Bulk density decreased significantly with increasing temperature and number of cycles, with cumulative reductions of up to 9.8% for AK soil and 7.6% for IP soil after five cycles at 500 °C. Atterberg limits decreased consistently with thermal cycling, accompanied by a reduction in fines and a corresponding increase in sand-sized particles. Swell potential decreased sharply after the first heating cycle and showed little change thereafter, while collapse potential decreased by more than 50% after initial heating, with no consistent trend in subsequent cycles. Unconfined compressive strength decreased significantly for both soils, with strength loss more pronounced in IP soil (up to 97% at 500 °C) than in AK soil (up to 59%). Overall, the results show that cyclic heating induces irreversible changes in lateritic soils, with the extent and persistence of change controlled by mineral composition, temperature level, and heating history. These findings are relevant to the engineering assessment of soils exposed to high-temperature events such as wildfires and thermal remediation.

Keywords Temperature fluctuations · Soil mineralogy · Microstructure · Thermal cycle · Geotechnical properties

Introduction

Soil properties play a critical role in a wide range of engineering applications, and there is increasing recognition that temperature variations can significantly change the mechanical, hydraulic, and physicochemical behavior of soils [1–6]. Consequently, thermo–hydro–mechanical interactions in soils have attracted growing attention in geotechnical engineering, particularly in contexts such as energy geostructures, underground power cables, nuclear waste repositories, round improvement techniques involving heat transfer and even wildfire management [7–10].

At low to moderate temperatures, most research has examined how soils respond to heating under controlled stress conditions. In these studies, temperature changes

✉ Lekan Olatayo Afolagboye
lekan.afolagboye@eksu.edu.ng; afotayour@hotmail.co.uk

Olubunmi Oluwadare Owoyemi
lade.owoyemi@gmail.com

Megan Welman-Purchase
purchasemd@ufs.ac.za

1 Department of Geology, Faculty of Pure and Applied Science, Kwara State University, Malete, Nigeria

2 Department of Geology, Faculty of Science, Ekiti State University, Ado-Ekiti, Nigeria

3 Department of Geology, University of Free State, Bloemfontein, South Africa

4 Department of Geology, Federal University, Oye -Ekiti, Nigeria

Published online: 11 March 2026

affect pore water viscosity, permeability, consolidation rates, and effective stress. For instance, recent studies on thermal consolidation shows that moderate heating can accelerate consolidation in soft soils by improving drainage and accelerating pore pressure dissipation, thereby reducing treatment time [11, 12]. These studies are generally conducted at temperatures below those that cause mineral alteration, allowing researchers to focus on how heat affect the hydraulic and mechanical behaviour of soils during ground improvement. However, they mainly address reversible or stress-related thermal effects and pay little attention to permanent changes in soil mineralogy or microstructure.

Beyond ground improvement and energy-related applications, thermal treatment is also used at much higher temperatures for remediating contaminated soil. In thermal remediation, soils are intentionally heated to remove or destroy pollutants [13–15]. Methods such as thermal desorption, thermal conduction heating, radio-frequency heating, and in-pile treatment typically raise soil temperatures above 300 °C and, in some cases, beyond 500 °C [16–20]. In extreme situations such as smoldering fires or incineration, soil temperatures can increase to about 1200 °C [21–23]. At these temperature levels, soil behaviour or response is no longer govern mainly by changes in pore fluids but also by dehydration, mineral breakdown, phase transformation, and particle agglomeration. These processes can permanently alter soil structure and lead to changes in its engineering behavior [24–26].

In addition to engineered thermal treatments, uncontrolled heating events such as wildfires and bush burning also expose soils to high temperatures, often in unpredictable ways. The increasing frequency and intensity of wildfires, driven by climate change, has made understanding their effects on soil properties a pressing concern properties [27–29]. Depending on fire intensity, duration, and soil conditions, temperatures in affected soils can range from about 200 °C to over 800 °C [9, 30–32]. In many tropical regions, including parts of sub-Saharan Africa, bush burning is a common practice that repeatedly heats near-surface soils. Despite how widespread this exposure is, the long-term effects of repeated high-temperature cycles on soil properties and engineering behavior are still poorly understood.

Most previous studies on thermal effect on soils have focused on single heating events or steady temperature changes, often using fine-grained soils from temperate regions [33–38]. While these studies have improved our understanding of thermal sensitivity of soils, they do not adequately capture the conditions associated with repeated heating and cooling cycles. In addition, they do not account for the distinct mineralogical characteristics of residual soils such as lateritic soil, which are rich in iron oxides and other minerals such as kaolinite, and feldspars. It is expected that the response of lateritic soil to elevated temperature to be different to that of sedimentary clay due their mode of formation, cementation and mineral assemblages.

Although studies on thermal consolidation [11, 12] show useful effects of moderate heating under controlled loading conditions, their findings, however, cannot be apply cyclic heating at higher temperatures. In these scenarios, minerals become unstable or mineral transformation may take place and the soil may undergo permanent structural changes that fundamentally alter its behaviour [39, 40]. This leaves a significant gap as there is still limited understanding of how repeated exposure to moderate and high temperatures affect the mineralogy, internal structure, and engineering properties of lateritic soils.

To address this gap, the objective of this study is to investigate the effects of repeated thermal exposure on the physical, mechanical, and microstructural properties of lateritic soils from southwestern Nigeria. Cyclic heating and cooling at 300 °C and 500 °C are applied to simulate high-temperature thermal disturbance scenarios such as thermal remediation and wildfire-affected soils. Through mineralogical analysis, microstructural observations, and standard geotechnical testing, the study examines how temperature level, heating cycles, and mineral composition together influence long-term changes in lateritic soil behaviour. Unlike previous research focused on low-temperature consolidation under controlled stress conditions, single heating events, or steady temperature changes, this work investigates high-temperature cyclic conditions relevant to post-heating engineering assessment rather than soil improvement.

Materials and methods

This study utilized bulk samples of residual lateritic soils collected from depths of 1.5 m at two locations in southwestern Nigeria: Akerebiata (AK) and Ipetu (IP). This depth was chosen to minimize the influence of past surface disturbances on soil structure. The AK soil developed over migmatite gneiss, while the IP soil developed over biotite schist (Fig. 1). Both parent rocks belong to the Precambrian Basement Complex of Southwestern Nigeria.

The soil samples were air-dried at room temperature for three weeks to reach a constant weight. This method was chosen over oven drying at high temperatures (100 °C to 110 °C) because previous research has shown it can cause irreversible changes in properties of lateritic soils [39, 41, 42]. The mineralogy, geochemistry, and microstructure of the air-dried soil were analyzed using X-ray diffractometry (XRD), X-ray fluorescence (XRF), and scanning electron microscopy (SEM), respectively. Physical and geotechnical properties such as natural moisture content, particle size

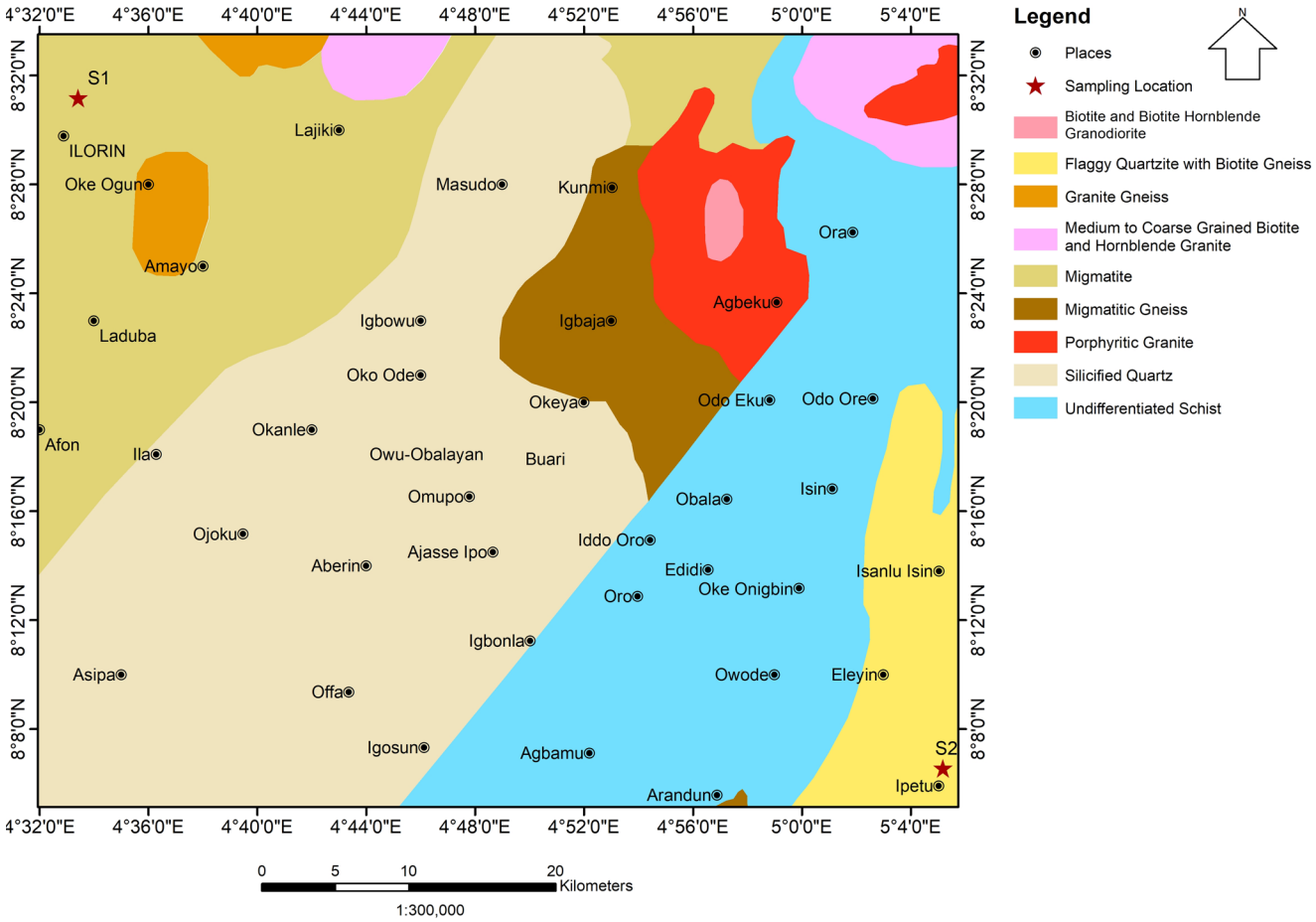


Fig. 1 Geologic map of the study area showing sampling locations

distribution, Atterberg limits, specific gravity, bulk density, compaction parameters (Standard Proctor), unconfined compressive strength, collapse potential, and swell potential were determined using standard methods. For the characterization of the soil samples, five replicate specimens were tested for each physical and geotechnical property, and the reported values represent the average of the five measurements.

The soil specimens were subjected to designated temperatures of 300 °C (moderate temperature) and 500 °C (high temperature) in an electric oven using a controlled heating rate of 5 °C/min. Heating was carried out on soil in a loose (uncompacted) state, placed in heat-resistant ceramic crucibles as shallow layers to promote heat penetration. Care was taken to maintain a similar soil thickness for all heating runs. After reaching the target temperature, the samples were held for one hour to allow thermal equilibration and were then allowed to cool to room temperature inside the oven. This heating–cooling cycle was repeated five times.

Following each cycle, the heated soils were tested for Atterberg limits, sieve analysis, bulk density, collapse potential, swell potential, unconfined compressive strength, SEM, and XRD. Three specimens were tested for each geotechnical property such as Atterberg limits, grain size distribution, bulk density, collapse potential, swell potential, and unconfined compressive strength. The results reported are the average values for each temperature level and heating cycle. All specimens within each test group were prepared using the same procedures to ensure consistent comparison across temperatures and cycles. Tests like XRD and SEM were only repeated on the fifth cycle samples to observe cumulative changes in microstructure and mineralogy due to cyclic heating.

For the unconfined compression test, swell potential test, and collapse potential test, thermal treatment was applied to the soil in a loose (uncompacted) state. After each heating–cooling cycle and removal from the oven, the soil was allowed to cool further in a desiccator and was then re-mixed with distilled water to restore its optimum moisture content (OMC), as determined from the Standard Proctor test on the natural soil. The soil was then compacted to its maximum dry density to produce the test specimens. This heat-then-compact sequence was applied consistently at both temperature levels and across all heating cycles. The approach was

chosen to reflect field conditions in which soils are exposed to heat before loading or being considered for engineering use, while maintaining consistent preparation across all tests (conditions). The geotechnical properties of the air-dried soil were compared to those of the heated samples after each cycle to evaluate the impact of the treatment. The observed changes were analyzed in relation to factors like geology, temperature regime, soil composition, and heating cycles.

Natural moisture content, specific gravity, bulk density, compaction, swell potential and consistency limits were determined according to [43]. The pycnometer method was used for specific gravity, while a graduated cylinder was used for bulk density. Grain size distribution analysis followed the standard test method outlined by [44]. Particles smaller than 423 μm were used for liquid and plastic limit determinations using the Casagrande method. Standard Proctor compaction energy and mold were employed for compaction parameter testing. Unconfined compression tests, collapse potential, and swell potential were conducted on compacted samples prepared at optimum moisture content and maximum dry density. The unconfined compression test was performed under controlled axial strain at a constant rate 1.5% per min, following [45]. The same loading rate was used for all specimens, irrespective of temperature level or number of heating cycles. For the swell test, specimens were placed under a small seating pressure of about 7 kPa and then flooded with water, allowing them to expand freely. The deformation was recorded until it stabilized, which typically occurred within approximately 24–48 h. For the collapse test, each specimen was first loaded with a constant vertical stress and then flooded with water while the load was maintained. Vertical deformation was measured over time.

For X-ray diffraction analysis, a Panalytical Empyrean diffractometer with a theta-theta goniometer configuration was used, scanning samples between 3.5° and 70° 2θ at tube settings of 45 kV and 40 mA. Data was collected using Collector v. 3.0c and Highscore v. 3.0e software with the ICDD PDF-2 database for diffractogram evaluation. Elemental analysis, excluding sodium, was conducted using a fusion disc method. Sodium was measured using a pellet disc. The disc preparation involved devolatilization at 110 °C followed by ignition at 1050 °C to determine the total loss or gain on ignition. A flux mixture was then added to the sample before heating to 950 °C for 5 min to form a molten liquid within a Pt crucible. This liquid was cast into a mold and pressed into a disc, followed by additional pressing at high pressure. Measurements were taken using Rigaku Primus X-ray fluorescence equipment. SEM microstructural analysis was performed on carbon-coated samples using a scanning electron microscope with backscatter electron imaging. Energy dispersive X-ray spectrometer (EDS JED-2300) detectors determined the elemental composition of the soil samples, with analysis conducted using NSS3 microanalysis software. The accelerating voltage was set at 20 kV, with an EDS detection limit of 100 ppm.

Statistical analyses were used to assess how thermal cycling and temperature influenced the measured soil properties. One-way ANOVA evaluated differences among heating cycles at a fixed temperature, while two-way ANOVA examined the effects of cycle number, temperature, and their interaction. All tests were based on replicate measurements, with significance assessed at the 5% level ($\alpha = 0.05$). When significant effects were identified, Tukey's Honestly Significant Difference (HSD) test was applied to identify pairwise differences between cycle means. Results are presented using letter groupings, where values sharing the same letter are not statistically different.

Table 1 Physical characteristics of the soils

Property	AK	IP
Natural moisture content (%)	18.5 ± 0.24	5.7 ± 0.16
Specific gravity	2.40 ± 0.02	2.73 ± 0.01
Gravel (%)	2 ± 0.71	2 ± 1.22
Sand (%)	49 ± 1.0	50 ± 0.71
Fines (%)	49 ± 1.58	48 ± 1.73
Bulk density (kg/m³)	1882 ± 5.7	1410 ± 3.81
Liquid limit (%)	45 ± 1.58	38 ± 1.22
Plastic limit (%)	25 ± 0.71	24 ± 1.58
Plasticity index (%)	20 ± 1.41	14 ± 1.22
Maximum dry density, MDD (kg/m³)	1960 ± 3.54	1748 ± 3.08
Optimum moisture content, OMC (%)	22.2 ± 0.19	16.8 ± 0.16
Collapse potential (%)	6.86 ± 0.23	5.9 ± 0.10
Swell potential (%)	−2.48 ± 0.15	−2.74 ± 0.08
Unconfined compressive strength (kPa)	256 ± 3.81	76.6 ± 1.14
USCS classification	CL	CL

Results and discussion

Properties of the natural soils

Prior to thermal treatment, both AK and IP soils were characterized to establish their baseline geotechnical properties. Table 1 summarizes the index and geotechnical properties, while Fig. 2 presents the particle size distribution curves. Both soils are classified as well-graded with a predominance of fine particles. Notably, AK soil exhibits higher plasticity and natural moisture content compared to IP soil. This suggests a greater presence of clay minerals in AK soil, potentially contributing to its higher collapse potential and greater susceptibility to sudden volume reduction upon wetting. The unconfined compressive strength of AK soil was significantly higher than that of IP soil, classifying them as very stiff clay and soft clay, respectively, based on the undrained shear strength criteria [46].

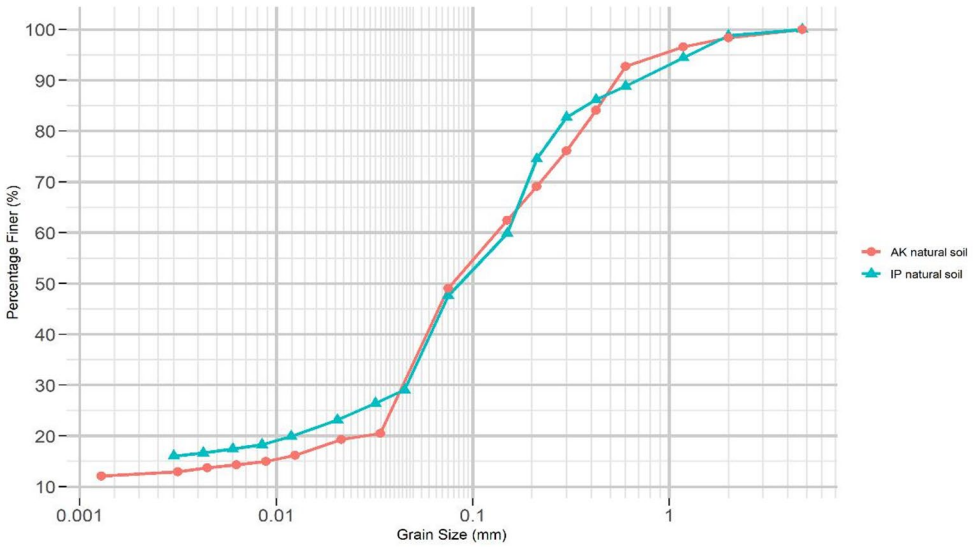


Fig. 2 Grading curves of the soil samples in their natural state

Table 2 Mineral composition of the natural and heated samples soil samples

Soil	Relative content: %						
	Quartz	Kaolinite	Goethite	Plagioclase	K-feldspar	Calcite	Ilmenite
AK_N	28	6		54	7	4	1
AK_500	39	4		29	27		1
IP_N	54	43	3				
IP_500	51	44	5				

*AK_N (Akerebiata natural soil), AK_500 (Akerebiata soil heated to the fifth cycle at 500 °C), IP_N (Ipetu natural soil), IP_500 (Ipetu soil heated to the fifth cycle at 500 °C)

The relatively small standard deviations for most parameters (Table 1) show minimal test variability, indicating that the mean values reliably represent the soils' properties. Moreover, the differences between AK and IP soils for key properties such as natural moisture content, plasticity index, bulk density, and unconfined compressive strength are substantially larger than their respective standard deviations, implying that these differences are systematic rather than arising from random variability.

X-ray diffraction (XRD) analysis revealed that IP soil is primarily composed of quartz and kaolinite, while AK soil has a more diverse mineralogical assemblage dominated by feldspars and quartz (Table 2).

This difference is reflected in the geochemical composition (Table 3). Both soils are rich in silica (SiO_2) and alumina (Al_2O_3). Notably, the alumina content is higher in the feldspar-rich AK soil compared to the kaolinite-rich IP soil, as feldspars are a significant source of alumina [47]. The combined content of iron, titanium, and aluminum oxides (sesquioxides) is also higher in AK soil (31.1%) compared to IP soil (20.3%). This aligns with the observed lower silica content in AK soil compared to IP, as sesquioxides can coat and bind silica particles.

[1]Oxide compositions, except for Na_2O, are reported on an ignited, loss-free basis. Loss on ignition (LOI) represents the mass lost after heating the sample to 1050 °C. Na_2O was measured separately using pellet discs prepared from unignited material. The total composition reflects the sum of these components, which are reported on different mass bases.

The X-ray diffractograms for the natural soils (Fig. 3) support these findings. Scanning electron microscopy (SEM) images (Fig. 4) provide visual evidence of the differences between the natural soils. AK soil exhibits a microstructure with larger particles, possibly due to the aggregation of finer particles caused by the higher concentration of sesquioxides. These inherent variations in both the geotechnical properties and mineralogical composition will likely influence how the soils respond to thermal treatment.

Effect of cyclic heat treatment on the mineralogy and microstructure of the soils

The comparison of mineralogy between natural soils and those subjected to five heating cycles at 500 °C (Table 2) reveals significant changes in the AK soil, while the IP soil remains relatively stable. It should be noted that metakaolin formed during heating (dehydroxylation) is largely amorphous and may not be easily detected by conventional XRD.

Table 3 Elemental composition of the natural soils

Soil	SiO_2	TiO_2	Al_2O_3	Fe_2O_3	MgO	MnO	CaO	Na_2O	K_2O	P_2O_5	LOI	Total
AK	59.1	2.1	22.1	6.9	0.3	0.1	2.6	0.3	0.8	0.0	7.6	101.9[1]
IP	66.0	0.6	19.6	6.9	0.0	0.1	0.2	0.0	0.5	0.0	7.6	101.4[1]

As a result, the kaolinite contents reported represent only the remaining crystalline fraction of the material, rather than the full aluminosilicate content or phase.

The mineral constituents of the IP soil, primarily kaolinite and quartz, exhibit greater thermal stability compared to the feldspars in AK soil. In the AK soil, the quartz content increased, the plagioclase feldspar content decreased, and the K-feldspar content increased distinctly (Fig. 3). Additionally, the trace amounts of calcite in AK soil disappeared. This is expected as plagioclase and calcite, both rich in calcium, are prone to breakdown at high temperatures through processes like calcination or decarbonation [48, 49]. This suggests that calcination or decarbonation, triggered by temperature cycling, likely occurred during the heating cycle.

Microstructural analysis after five heating and cooling cycles shows similar changes in both soil samples (Fig. 4). The particles became larger and more rounded due to agglomeration, with a higher degree of agglomeration observed in samples heated to 500 °C. This indicates that higher temperatures enhance particle coalescence and rounding, likely affecting the soil's mechanical properties. The observed agglomeration can be attributed to the breakdown of some minerals and the subsequent fusion or re-precipitation of their constituents around existing particles during the heating process, a phenomenon driven by high temperatures promoting increased particle interaction and fusion, leading to the formation of larger, more rounded structures.

Although direct porosity measurements were not performed, the observed decrease in bulk density indicates an increase in total porosity. Furthermore, the particle agglomeration visible in SEM micrographs and the corresponding shift in grain size distribution as well as the measured changes in compaction behaviour and collapse potential, suggest significant thermally induced pore rearrangement and fabric modification, including a coarsening of the pore network, during cyclic heating. While particle agglomeration is qualitatively evident from SEM images and grain-size trends, this study did not include quantitative measures such as fractal analysis or image-based particle characterization. Future work using these approaches would provide direct metrics to better integrate microstructural changes into constitutive models.

These observations suggest that the mineralogical and microstructural stability of the IP soil under cyclic heating can be attributed to its quartz and kaolinite composition, which resist thermal alteration. In contrast, the AK soil's mineralogical transformation, especially the reduction of plagioclase and disappearance of calcite, underlines the vulnerability of calcium-rich minerals to high-temperature processes. The resulting changes in AK soil's mineral composition and microstructure have potential implications for

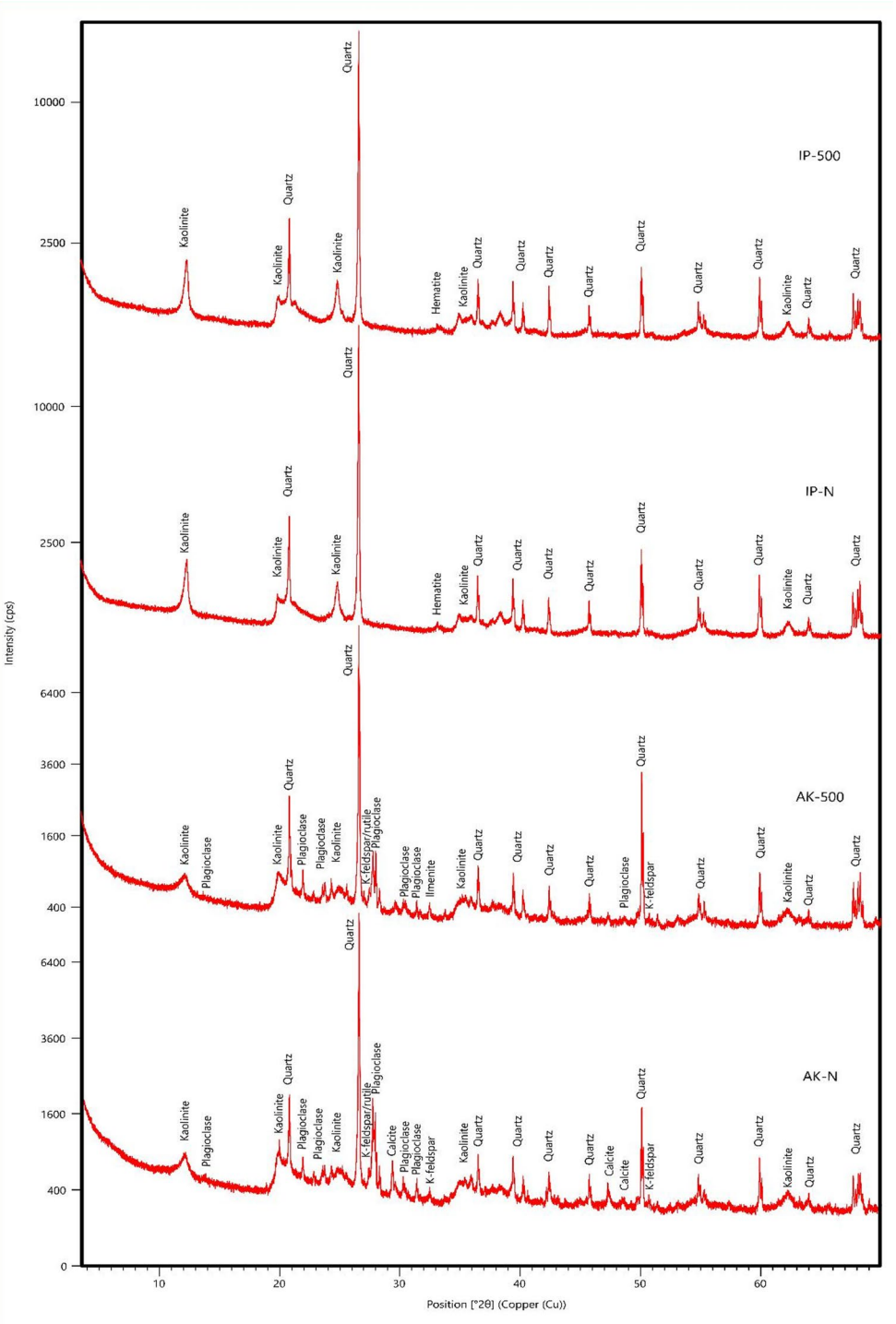


Fig. 3 X-Ray diffractograms of the natural and thermally recycled soils at 500 °C

its geotechnical performance post-heat treatment. The disappearance of calcite and reduction of plagioclase in AK soil may lead to a decrease in soil strength and stability, as the reduction of calcium-rich minerals can weaken the soil matrix, making it less capable of maintaining structural integrity under load [48]. On the other hand, the increase in quartz and K-feldspar may enhance properties like thermal stability. Quartz and K-feldspar, known for their high melting points and resistance to thermal stress, can improve the soil's performance in high-temperature environments [49]. The rounding and enlargement of particles due to agglomeration can affect soil compaction and permeability, as larger, more rounded particles reduce the soil's capacity to compact densely, leading to higher permeability and lower load-bearing capacity [50].

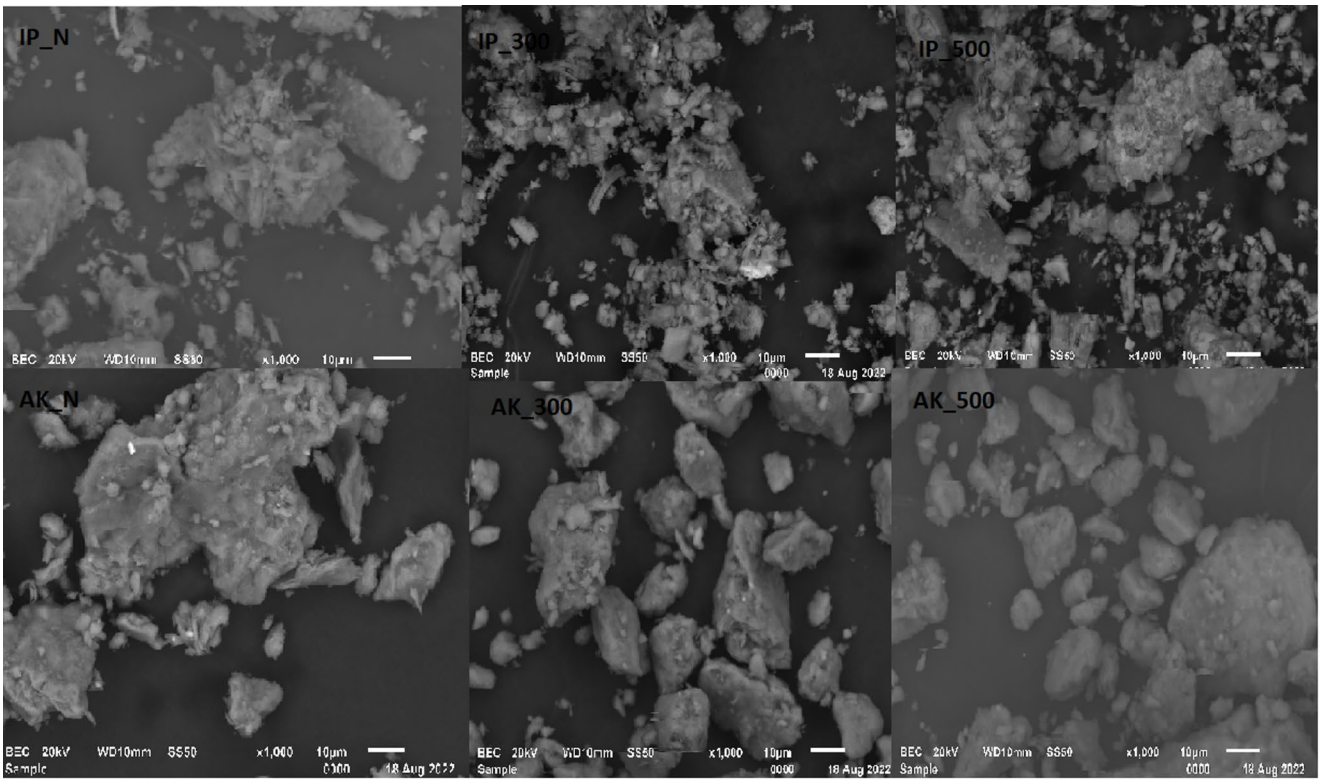


Fig. 4 Scanning electron microscopy of the natural and heated samples AK_N (Akerebiata natural soil), AK_500 (Akerebiata soil heated to the fifth cycle at 500 °C), IP _N (Ipetu natural soil), IP_500 (Ipetu soil heated to the fifth cycle at 500 °C)

While direct SWCC measurements were not performed, the observed reductions in bulk density, plasticity, and strength, together with microstructural evidence of particle aggregation, suggest that thermal cycling would alter the hydraulic retention behaviour of the soils. Changes in pore size distribution and soil fabric are known to influence the soil-water characteristic curve, particularly the air-entry value and water retention capacity [51–53]. Within established thermo–hydro–mechanical frameworks for unsaturated soils, such fabric coarsening and density reduction are therefore expected to reduce air-entry values and suction-related stiffness, leading to modified suction–deformation responses under field conditions [54]. Future studies incorporating direct SWCC and suction measurements would allow these inferred trends to be tested and quantified.

Effect of the heating cycle on the geotechnical properties of the soils

Bulk density

Cyclic heating led to a decrease in bulk density for both soils at both 300 °C and 500 °C (Fig. 5). This decrease became more pronounced with an increasing number of heating cycles. Notably, the most significant reduction occurred after the first cycle, and the higher temperature (500 °C) consistently resulted in a greater decrease in density compared to 300 °C across all cycles. Specifically, after the fifth cycle, the cumulative percentage decrease in bulk density was 7.6% for IP soil and 9.8% for AK soil. The feldspar-rich AK soil experienced a greater reduction in bulk density compared to IP soil. The decrease in bulk density is more influenced by the temperature cycle and intensity than by the soil type (Fig. 5). This suggests that the cyclic heating effects on bulk density are primarily driven by the thermal stress and the number of heating cycles rather than the specific mineralogical composition of the soil.

The observed decrease in bulk density can be attributed to the loss of volatiles such as water and organic materials during heating. As these components are expelled from the soil matrix, the overall volume of the soil increases, leading to a reduction in bulk density. This phenomenon is consistent with findings in other studies where thermal treatment causes dehydration and decomposition of organic matter, resulting in changes in soil structure and density [37, 48]. The lower bulk density at higher temperature treatment can signify increased porosity, which can impact factors like water infiltration, soil strength, and overall stability.

The one-way ANOVA results (Table 4) show that the number of thermal cycles has a statistically significant effect on bulk density for both soils at each temperature (F_{CAL}

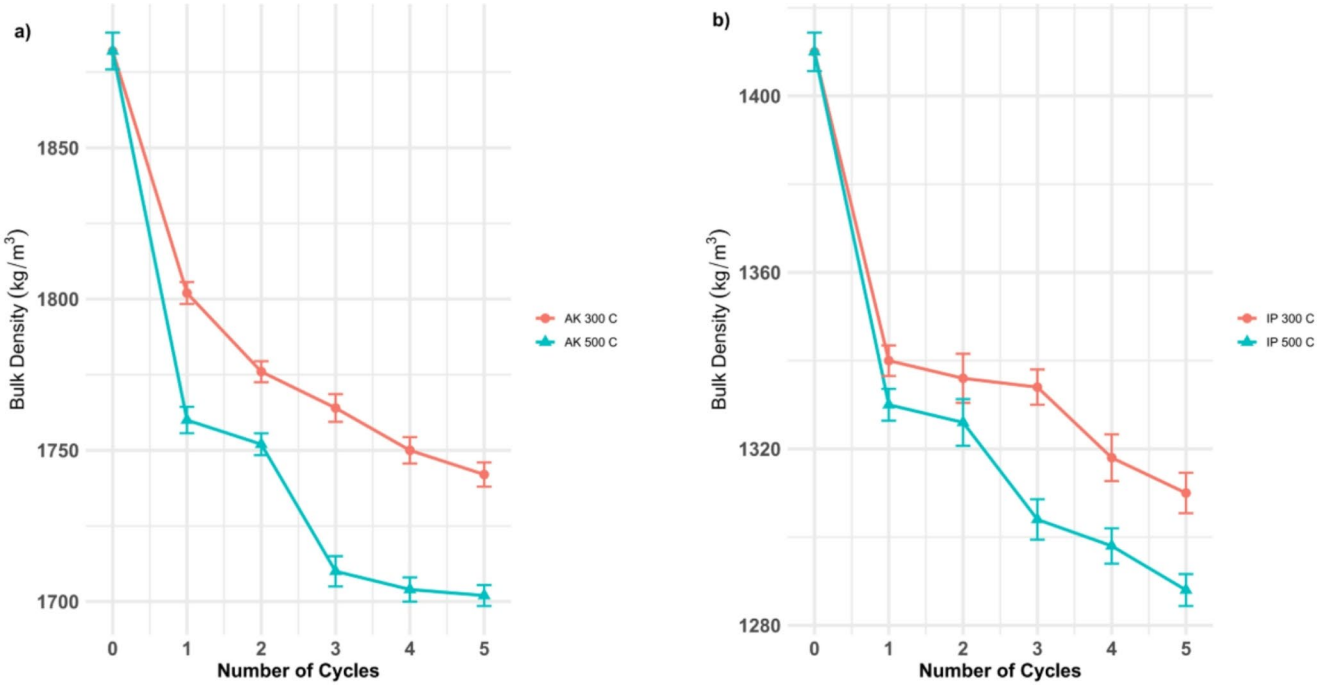


Fig. 5 Variation of Bulk Density with Heating Cycle **a** AK Soil **b** IP Soil

> F_{CRIT}). For example, at 500 °C, bulk density decreases significantly with increasing cycles for both AK (F_{CAL} = 405.40 > F_{CRIT} = 3.106) and IP soils (F_{CAL} = 320.20 > F_{CRIT} = 3.106), indicating progressive degradation as thermal cycling increases. Tukey's HSD tests (Table S1) reveal that the pattern of change varies with soil type and temperature. For AK soil at 300 °C, each cycle differs significantly from the previous one ($p < 0.05$), except for cycles 4 and 5, which are statistically similar. This suggests that degradation slows and begins to stabilize at higher cycle numbers. At 500 °C, AK soil shows significant differences between early and later cycles, but not between cycles 1 and 2 or cycles 4 and 5, indicating initial degradation followed by stabilization. For IP soil at 300 °C, cycles 1 to 3 are statistically similar, while cycles 4 and 5 form a distinct lower group, confirming progressive degradation with repeated heating. At 500 °C, IP soil displays four statistically distinct groups across the cycles, with a steady reduction in bulk density and no clear evidence of stabilization at higher cycles.

The two-way ANOVA results (Table S2) further confirm these trends. For AK soil, both cycle number (F_{CAL} = 1076.09 > F_{CRIT} = 2.621) and temperature (F_{CAL} = 530.45 > F_{CRIT} = 4.260) have strong and significant effects on degradation. A significant interaction between cycle number and temperature (F_{CAL} = 28.49 > F_{CRIT} = 2.621) indicates that degradation progresses more rapidly at 500 °C than at 300 °C. For IP soil, cycle number (F_{CAL} = 480.7 > F_{CRIT} = 2.621) and temperature (F_{CAL} = 107.1 > F_{CRIT} = 4.260) also have significant effects, with a weaker but still significant interaction (F_{CAL} = 8.71 > F_{CRIT} = 2.621). Together, these results show that both repeated heating and higher temperature drive bulk density loss, with stronger and more persistent effects at 500 °C.

Atterberg limits and grain size distribution

Figure 6 presents the Casagrande classification chart for the two soils, illustrating the effect of cyclic heating on their consistency limits. Cyclic heating resulted in a consistent decrease in both the liquid limit and plastic limit of the soils (AK and IP), regardless of the number of heating cycles or soil type (Fig. 6). This trend is reflected in the Casagrande classification chart, where the heated soils exhibited a shift towards lower plasticity classifications. Notably, soils heated to 500 °C exhibited a more significant reduction in plasticity compared to those heated to 300 °C. For example, some IP soil specimens originally classified as medium plasticity clays transitioned to low plasticity clays at higher heating temperatures. Similarly, two AK samples heated at 500 °C displayed a shift from medium plasticity clays to low plasticity silts during the fourth and fifth cycles. These observations suggest a transformation in soil behaviour from being dominated by finer particles to a more coarse-grained particles or towards a less plastic state. This observation can be attributed to particle agglomeration, where finer soil particles cluster together to form larger ones. This is further supported by changes in the grain size distribution of the soils (Fig. 7) and the microstructural analysis. Both soils

Table 4 One-way ANOVA results for the properties of the soils

Property	Soil	Temp	F_{CAL}	*P*- value	F_{CRIT}	Remarks
Bulk Density (Kg/m^3)	AK	300° C	405.4	6.05E-13	3.106	Significant
	AK	500° C	694.4	2.44E-14	3.106	Significant
	IP	300° C	179.3	7.65E-11	3.106	Significant
	IP	500° C	320.2	2.46E-12	3.106	Significant
Liquid Limit (%)	AK	300° C	178.8	3.85E-11	3.106	Significant
	AK	500° C	647.1	3.72E-14	3.106	Significant
	IP	300° C	122.3	7.26E-10	3.106	Significant
	IP	500° C	520	1.37E-13	3.106	Significant
Plastic Limit (%)	AK	300° C	81.65	7.66E-09	3.106	Significant
	AK	500° C	2069.92	3.53E-17	3.106	Significant
	IP	300° C	68.53	2.11E-08	3.106	Significant
	IP	500° C	69.95	1.87E-08	3.106	Significant
Sand (%)	AK	300° C	97.7	2.7E-09	3.106	Significant
	AK	500° C	158.9	1.56E-10	3.106	Significant
	IP	300° C	317.6	2.58E-12	3.106	Significant
	IP	500° C	123.6	6.83E-10	3.106	Significant
Fine (%)	AK	300° C	23.91	7.47E-06	3.106	Significant
	AK	500° C	36.8	7.12E-07	3.106	Significant
	IP	300° C	72.73	1.5E-08	3.106	Significant
	IP	500° C	28.125	3.12E-06	3.106	Significant
Swell Potential (%)	AK	300° C	1481.47	2.62E-16	3.106	Significant
	AK	500° C	2372.58	1.56E-17	3.106	Significant
	IP	300° C	162.32	1.38E-10	3.106	Significant
	IP	500° C	911.94	4.78E-15	3.106	Significant
Collapse Potential (%)	AK	300° C	379.77	8.92E-13	3.106	Significant
	AK	500° C	85.85	5.72E-09	3.106	Significant
	IP	300° C	101.19	2.2E-09	3.106	Significant
	IP	500° C	332.66	1.96E-12	3.106	Significant
UCS (kN/m^3)	AK	300° C	768.95	1.33E-14	3.106	Significant
	AK	500° C	667.98	3.07E-14	3.106	Significant
	IP	300° C	191.99	5.11E-11	3.106	Significant
	IP	500° C	270.92	6.65E-12	3.106	Significant

Source of Variation: Number of Cycle; Degree of Freedom: Between = 5; Within = 12

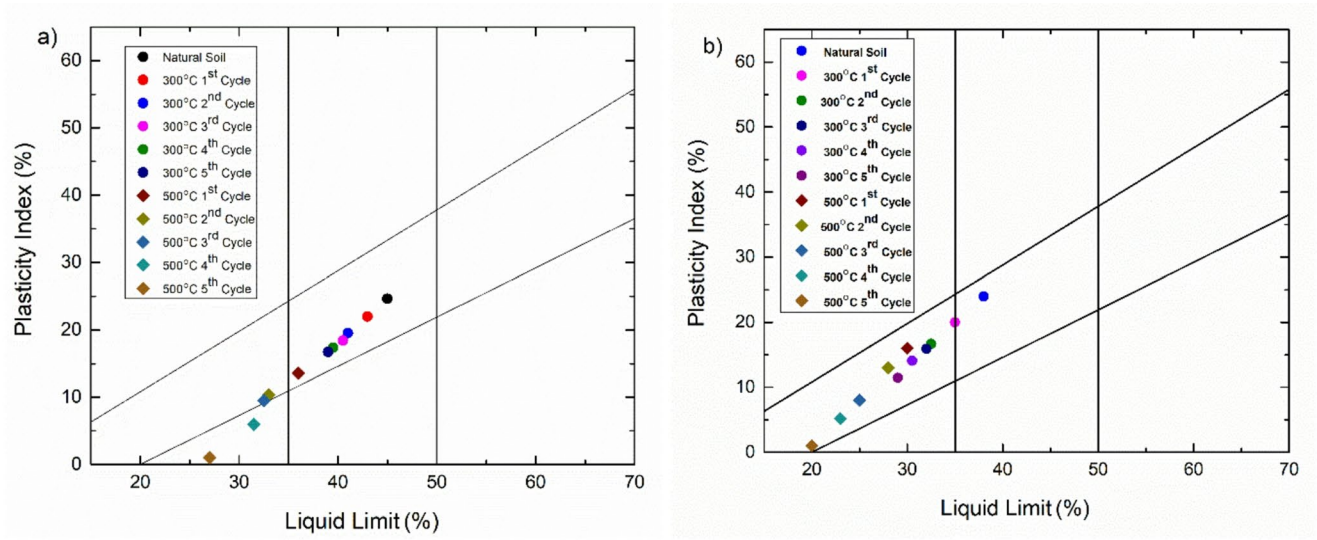


Fig. 6 Casagrande Chart showing classification of natural and heated soil samples. **a** AK Soil **b** IP Soil

displayed a decrease in the amount of fines (smaller particles) with a corresponding increase in sand-sized particles, indicative of particle aggregation due to the heat treatment.

One-way ANOVA (Table 4) showed that thermal cycling had a significant effect on the liquid limit of the AK soil at both temperatures. At 300 °C, the effect was statistically significant ($F = 178.8$, $p = 3.85 \times 10^{-11}$). Tukey's HSD test (Table S1) indicated similar liquid limit values between Cycles 2 and 3, and between Cycles 4 and 5, while all other cycles differed significantly. This pattern suggests a gradual change with signs of stabilization at higher cycle numbers. At 500 °C, the effect was even stronger ($F = 647.1$, $p = 3.72 \times 10^{-14}$). Tukey's test showed that Cycles 2, 3, and 4 were statistically similar, with Cycle 0 forming the highest group and Cycle 5 the lowest, indicating marked degradation followed by partial stabilization. Thermal cycling also had a significant influence on the liquid limit of the IP soil at both temperatures (Table 4). At 300 °C, one-way ANOVA confirmed a strong effect ($F = 122.3$, $p = 1.08 \times 10^{-9}$). Tukey's HSD test showed that most cycles differed from one another, except for Cycles 2 and 3, which were statistically similar (Table S1). Overall, the liquid limit decreased steadily from Cycle 0 to Cycle 5. At 500 °C, the effect was more pronounced ($F = 520.0$, $p = 4.55 \times 10^{-12}$). Tukey's test indicated that all cycles were significantly different, with a consistent and uninterrupted decline in liquid limit across cycles, showing no evidence of stabilization at the higher temperature. Similarly, two-way ANOVA (Table S2) revealed that liquid limit was significantly influenced by thermal cycle number, temperature, and their interaction for both AK and IP soils ($p < 0.05$). Together, these results demonstrate that repeated heating and increasing temperature jointly drive a progressive reduction in liquid limit, with the effect being more pronounced and persistent at 500 °C. One-way and

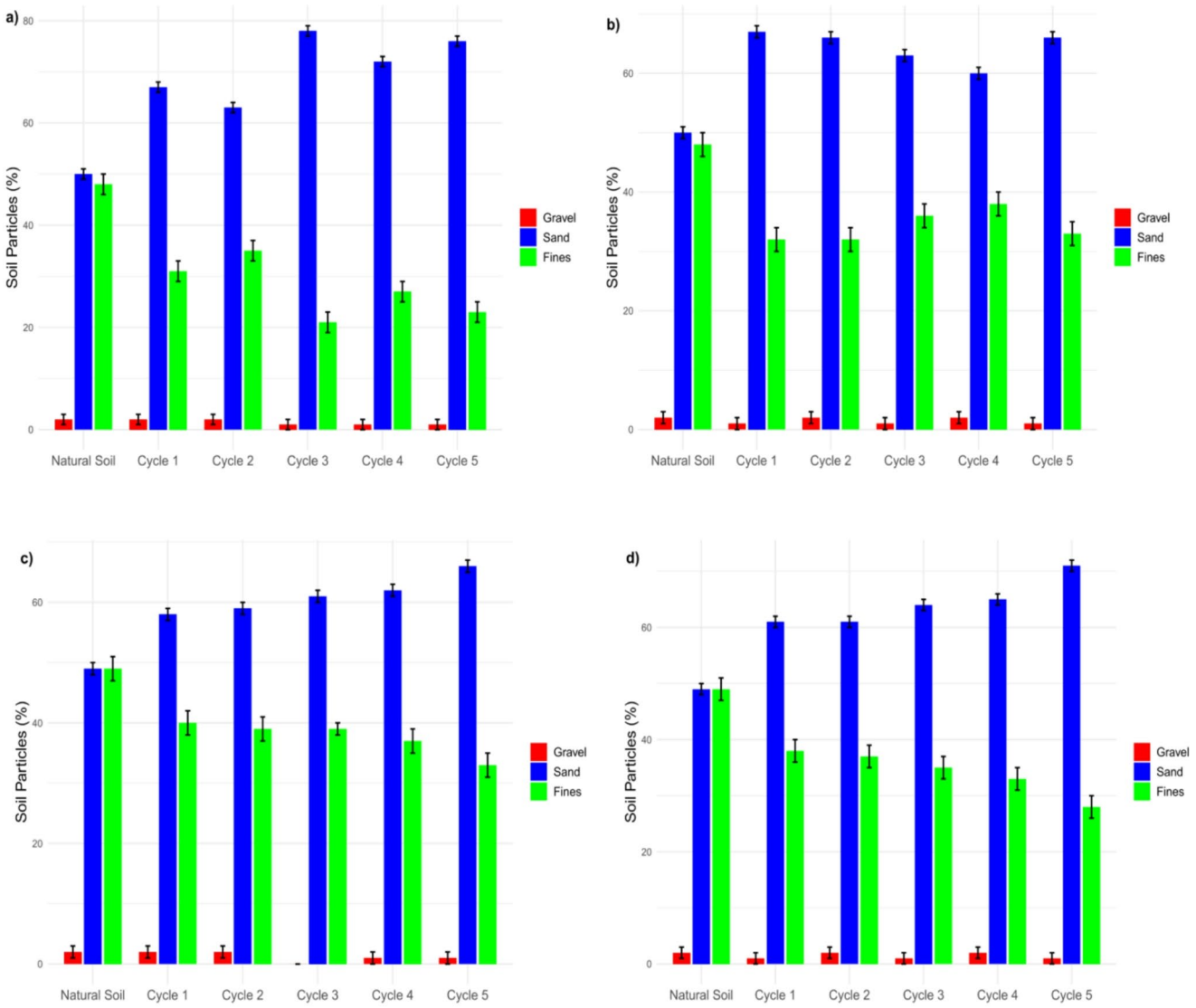


Fig. 7 Variation in the grain size distribution of natural and heated soils **a** IP-300 **b** IP-500 **c** AK-300 **d** AK-500

two-way ANOVA (Table 4 and Table S2) produced consistent results, confirming that plastic limit was significantly influenced by thermal cycling, temperature, and their interaction for AK and IP soils ($p < 0.05$). Tukey's HSD post-hoc analysis (Table S1) identified the same statistically significant differences and cycle groupings. The corresponding HSD results are summarized in Table S1.

One-way and two-way ANOVA (Table 4 and Table S2) show consistent results, confirming that sand and fine contents are significantly affected by thermal cycling, temperature, and their interaction in both AK and IP soils ($p < 0.05$). At 500 °C, for example, one-way ANOVA indicates that sand content changes significantly with increasing cycles for both AK ($F_{cal} = 158.9 > F_{crit} = 3.106$) and IP soils ($F_{cal} = 123.6 > F_{crit} = 3.106$), pointing to a progressive effect of repeated heating. Tukey's HSD results for sand and fine contents at both temperatures (Table S1) reveal a clear pattern across cycles. Early cycles form a distinct group, intermediate cycles partly overlap, and the final cycle mostly stands apart, reflecting a gradual shift with continued thermal exposure. For example, in AK soil at 500 °C, fine content in Cycle 0 differs significantly from all later cycles, while Cycles 1–3 overlap and the lowest values occur at Cycle 5. A similar trend is observed in IP soil at 500 °C, where Cycle 0 shows significantly higher fine content than all subsequent cycles, and later cycles cluster together, indicating a steady reduction with repeated heating.

The agglomeration of particles during cyclic heating can be explained by the breakdown of certain minerals and the subsequent fusion or re-precipitation of their constituents around existing particles. This process effectively reduces the overall surface area of the soil, a key factor influencing water adsorption and plasticity. The reduced surface area translates to a lower capacity for water retention, thereby lowering the liquid and plastic limits of the heated soils. In addition, the reduction in fines and increase in sand-sized particles can significantly impact the soil's mechanical behaviour, including its compaction characteristics and shear strength. The consistent reduction in the Atterberg limits, especially at higher temperatures, suggests a decrease in the soil's plasticity and workability. Lower plasticity soils are generally less compressible and exhibit reduced swell-shrink behaviour, which can be beneficial in engineering applications where stability and reduced deformation are important.

Swell potential

Moisture-induced volume changes can significantly impact the stability of residual soils [55]. Expansive soils, for instance, can swell upon wetting, leading to structural problems. On the other hand, collapsible soils exhibit a decrease in volume when wetted. Interestingly, the swell potential measured for both AK and IP soils was negative, signifying a tendency to shrink rather than swell when exposed to moisture. The variation in swell potential with the number of heating cycles displayed a similar pattern for both soils and heating temperatures (Fig. 8). There was a significant decrease in shrinkage potential after the first heating cycle, with subsequent cycles appearing to have minimal further effect. This suggests that the initial heat cycle has the most pronounced impact on the soil's shrinkage behaviour. In addition, the initial decrease in shrinkage potential also suggests that some of the mechanisms responsible for volume reduction upon wetting might be mitigated by the initial heat treatment. One-way ANOVA (Table 4) showed that thermal cycling had a strong and statistically significant effect on the swell potential of both AK and IP soils at 300 °C and 500 °C ($p < 0.0001$). Tukey's HSD results (Table S1) indicate that most of the reduction occurred during the initial cycles, particularly between Cycle 0 and the early heating stages. As cycling continued, changes became smaller, and the later cycles grouped into similar response levels, indicating stabilization at reduced swell potential. This pattern was more pronounced at 500 °C, where higher temperature led to a faster and more sustained reduction. Similarly, two-way ANOVA (Table S2) revealed that swell potential was significantly influenced by thermal cycle number, temperature, and their interaction for both AK and IP soils ($p < 0.05$).

The observed decrease in shrinkage potential after heating could be attributed to several factors. One possibility is the decomposition of clay minerals during heating, which can lead to a reduction in the soil's overall shrink-swell capacity. Additionally, the agglomeration of particles discussed earlier might contribute to a denser packing arrangement, limiting the potential for significant shrinkage upon wetting.

Collapse potential

In their natural states, both IP and AK soils exhibit collapse potentials at 200 kPa (collapse index) ranging between 5% and 7% (Fig. 9). According to [56], soils within this collapse range are considered potentially problematic. These values are generally lower than those reported by [55], which might be attributed to differences in parent rocks and mineralogical constituents of the residual soils studied. The first heating cycle, at both 300 °C and 500 °C, resulted in a significant reduction (at least 50%) in the collapse potential of both soils (Fig. 9). One-way ANOVA (Table 4) shows that thermal cycling has a strong and statistically significant effect on the collapse potential of both AK and IP soils at 300 °C and 500 °C ($p < 0.0001$). Tukey's HSD results (Table S1) indicate that most of the reduction occurs during

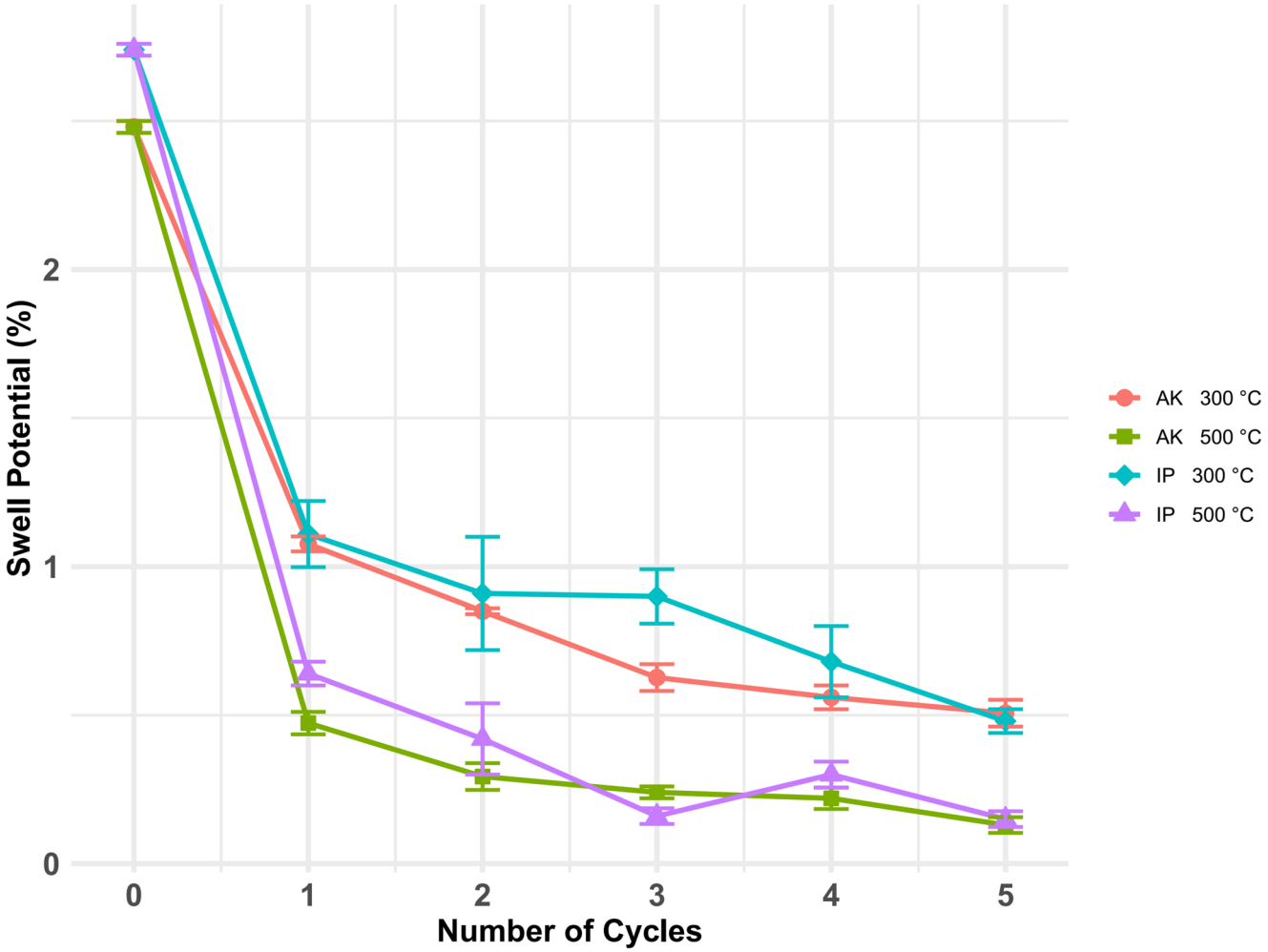


Fig. 8 Variation of swell potential of the soils with heating cycle

the initial cycles, particularly between the uncycled condition (Cycle 0) and the early heating stages. With continued cycling, changes become smaller and the later cycles group into statistically similar response levels, indicating stabilization at lower collapse potential. This effect is more pronounced at 500 °C, where the higher temperature leads to a greater and more sustained reduction than at 300 °C. Collapse potential in lateritic soils is controlled by a metastable fabric sustained by clay bridges, cementation, and interparticle bonding, rather than by density alone [57, 58]. Repeated heating and cooling progressively weaken these bonds through dehydration, mineral alteration, and thermally induced microcracking [59, 60]. As a result, although bulk density decreases with thermal cycling, the collapse-prone fabric is partially destroyed, leading to a reduced tendency for sudden collapse upon wetting. Similarly, two-way ANOVA (Table S2) revealed that collapse potential was significantly influenced by thermal cycle number, temperature, and their interaction for both AK and IP soils ($p < 0.05$).

This improvement reclassifies the soils from potentially problematic to those posing moderate concerns [56]. The reduction in collapse potential is likely due to the decrease in bulk density resulting from the heating cycle. However, after the first cycle, a clear trend in the collapse index with subsequent heating cycles was not evident. This suggests that other factors besides bulk density, such as matric suction [61], might play a more dominant role in influencing the collapse potential of these soils under cyclic heating conditions. Soils with reduced collapse potential are less likely to undergo significant volume reductions under loading, enhancing their stability and suitability for construction purposes.

Unconfined compressive strength

Unconfined compressive strength provides an estimate of the undrained shear strength of soils. Both IP and AK soils exhibit a reduction in strength after the first heating cycle at both 300 °C and 500 °C (Fig. 10). Subsequent heating

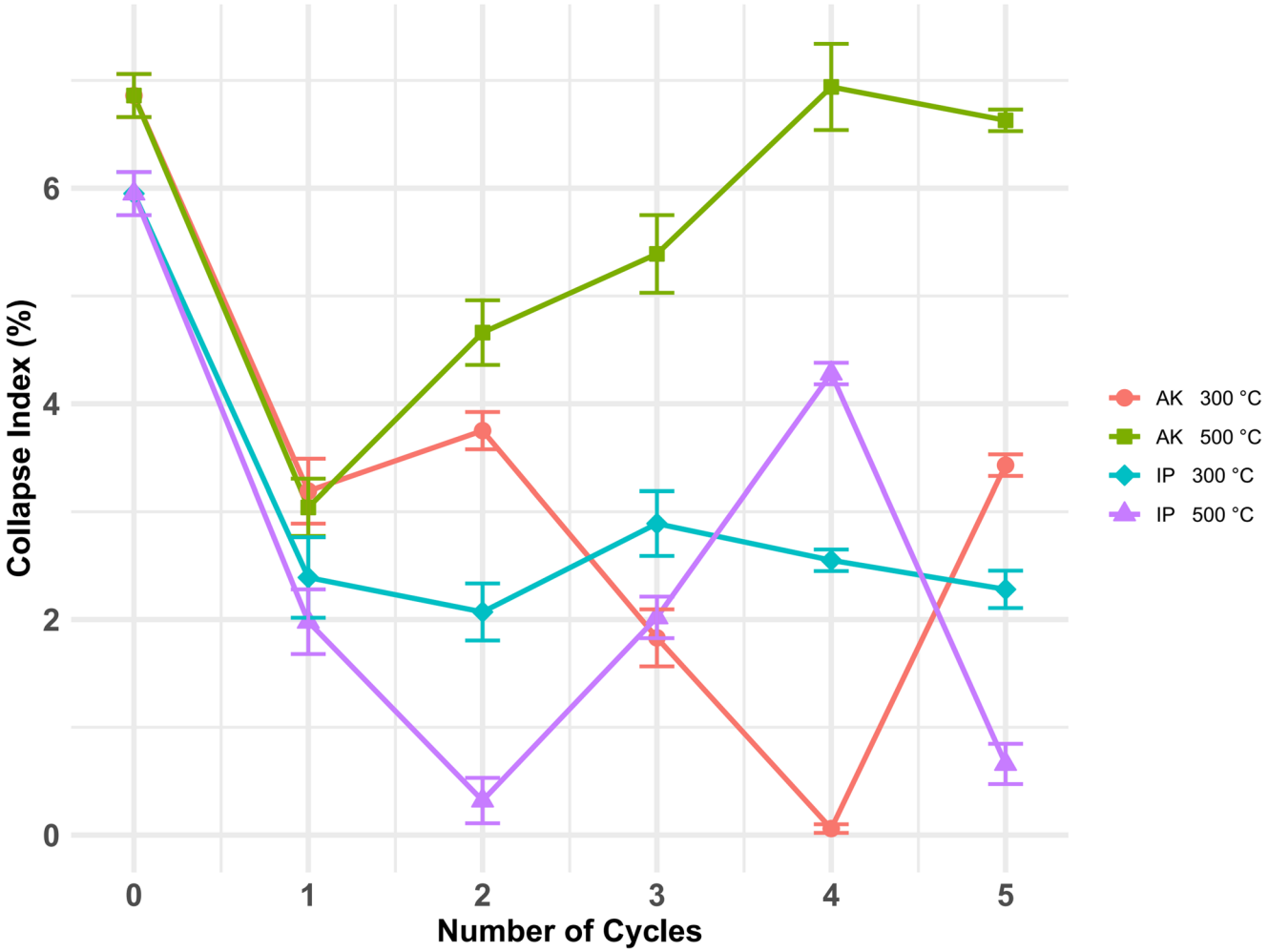


Fig. 9 Variation of collapse potential with heating cycles

cycles result in a continued but slower reduction in strength. The cumulative decrease in UCS at the end of the experiment (after five cycles) was significantly higher for IP soil compared to AK soil. At 300 °C, the strength reduction was 92% and 40% for IP and AK soils, respectively. Similarly, at 500 °C, IP soil exhibited a 97% decrease, while AK soil experienced a 59% decrease.

One-way ANOVA shows that thermal cycling (Table 4) has a strong and statistically significant effect on the unconfined compressive strength of both AK and IP soils at 300 °C and 500 °C ($p<0.001$). Tukey's HSD results indicate that most of the strength loss occurs during the initial cycles, particularly between the unheated condition (Cycle 0) and the early heating stages. As cycling continues, the rate of strength reduction decreases, and later cycles group into similar response levels, indicating stabilization at lower strength values. This pattern is observed in both soils but is more pronounced at 500 °C. For AK soil, the first cycle at 500 °C causes a sharp drop in strength, followed by smaller changes in subsequent cycles. IP soil shows a similar trend, with the highest strength in the uncycled state and progressively lower strengths after heating, eventually clustering at advanced cycles. Overall, higher temperature leads to greater and more persistent strength loss than at 300 °C. Similarly, two-way ANOVA (Table S2) revealed that undrained shear strength was significantly influenced by thermal cycle number, temperature, and their interaction for both AK and IP soils ($p<0.05$).

The observed reduction in unconfined compressive strength suggests that the initial strength of the soil, likely influenced by its mineralogical composition and cementation state, plays a role in the extent of strength reduction or thermally induced degradation. Heating at the higher temperature (500 °C) resulted in a greater overall decrease in strength for both soils. These findings differ from those reported by [41, 42], who observed an increase in strength for lateritic soils heated at a lower temperature (110 °C). The contrasting results may be attributed to the much higher temperatures and the repeated heating and cooling cycles

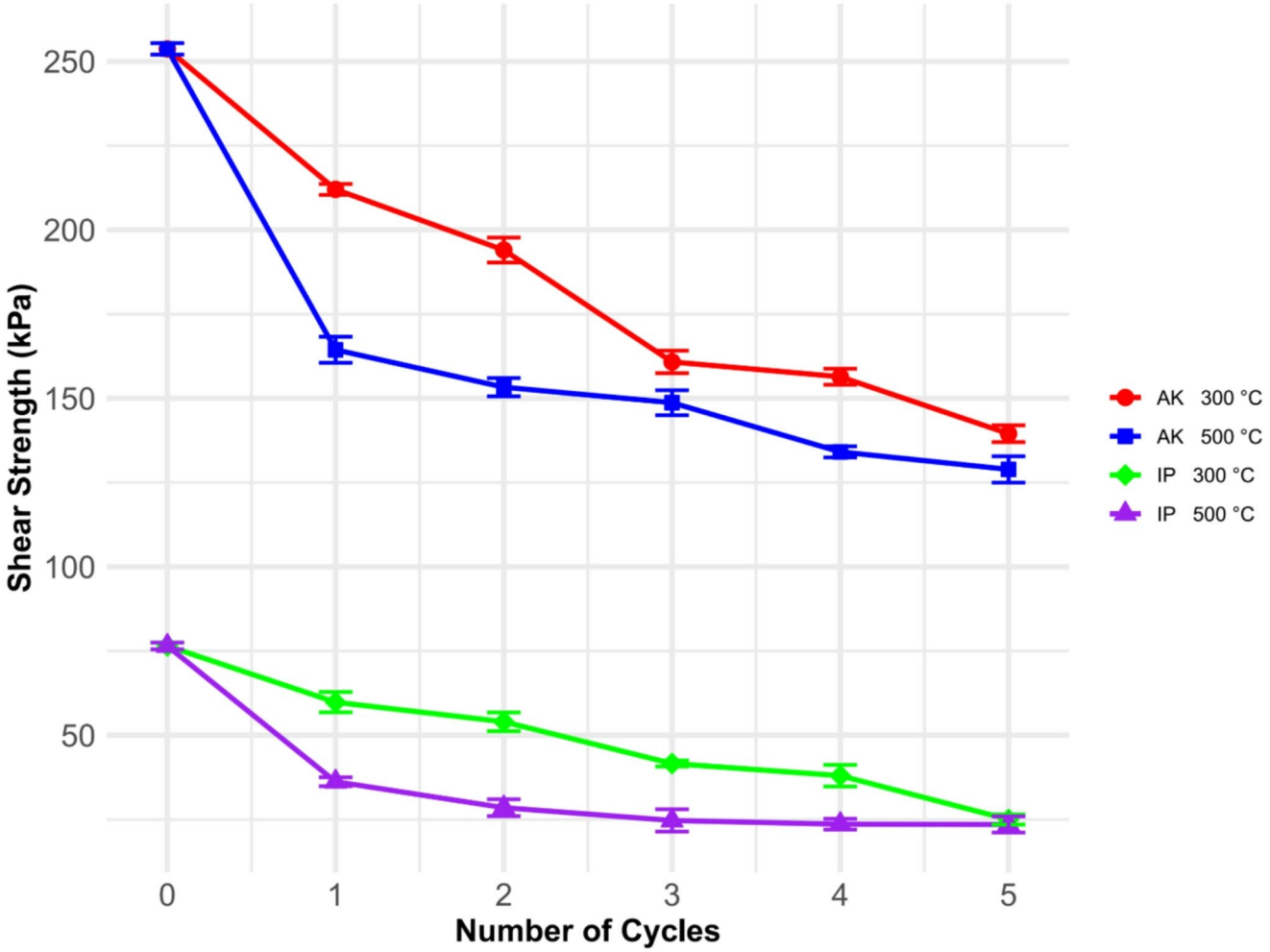


Fig. 10 Variation in unconfined compressive strength of the soil samples with heating cycle

used in this study, which promote progressive breakdown rather than temporary strengthening [62].

At both 300 °C and 500 °C, repeated heating and cooling likely cause the soil's mineral components to expand and contract at different rates. For instance, quartz grains, clay minerals and the surrounding iron–aluminum oxide cementing phases may expand and contract at different rates and temperature. This thermal mismatch creates stress at their boundaries, which promote microcracks initiation and weaken the soil structure over time. Similarly, differences in thermal behaviour and expansion across various crystallographic axes of the same mineral can induce thermal stresses [63].

The temperatures applied in this study align with known transformation ranges for key minerals in lateritic soils. Goethite begins to convert to hematite above about 250–300 °C, which weakens iron-oxide bonding and can also affect soil color and density. Kaolinite starts to break down above roughly 450 °C, forming largely amorphous metakaolin and leading to lower plasticity and weaker particle bonding [64]. By contrast, feldspars remain stable across the temperature range examined, and calcite breaks down only at much higher temperatures. Calcite decomposition is therefore unlikely to have contributed meaningfully to the changes observed in this study.

The SEM images, showing more rounded particles and increased aggregation, support this explanation and point to a gradual breakdown of the original bonded structure. From a microstructural perspective, repeated heating-cooling cycles causes accumulation of microcracks and progressively weakens the bonds or cementation between particles. This leads to a sharp drop in strength during the initial heating cycles. As damage accumulates, the soil structure gradually adjusts, and strength levels off at a lower, more stable state. The higher strength loss observed at 500 °C suggests more probable extensive mineral alteration and microstructural damage at higher temperature. As a result, the soil skeleton becomes less effective at carrying load, leading to more pronounced and lasting weakening.

Relevance to field thermal events

The observed changes in soil properties can be better understood by estimating the thermal energy applied during the tests. Using a representative soil heat capacity of about 800 $J \cdot kg^{-1} \cdot K^{-1}$ and the imposed temperature increases, the cumulative energy input after five cycles is on the order of $1–2 \times 10^6$ $J \cdot kg^{-1}$. This level of energy is comparable to that experienced by near-surface soils during intense wildfires or repeated thermal remediation activities. Although the laboratory heating represents a controlled, upper-bound scenario, it reflects severe but realistic field conditions. The resulting losses in strength and stability therefore have direct relevance for evaluating and potentially reusing lateritic soils that have been exposed to high-temperature events.

Conclusion

This study evaluated the effects of cyclic moderate (300 °C) and high (500 °C) temperature exposure on the mineralogical, microstructural, and geotechnical behaviour of lateritic soils from southwestern Nigeria. The results show that repeated heating and cooling cycles cause significant and mostly irreversible changes in soil properties. The extent of these changes depends on the soil's mineral composition, the temperature reached, and the number of heating cycles. Cyclic heating caused mineralogical changes in the feldspar-rich AK soil, while the kaolinite–quartz-dominated IP soil remained more stable. In both soils, thermal cycling led to particle agglomeration, reductions in bulk density, and a gradual shift toward coarser particle-size distributions. These changes were accompanied by reductions in Atterberg limits, indicating a loss of plasticity as temperature and heating cycles increased. Volume-change behaviour was mostly affected during the first heating cycle. Both swell and collapse potentials decreased sharply after the first cycle and then remained relatively stable. This suggest that early heat exposure which causes damage to metastable soil fabric plays a dominant role. In contrast, unconfined compressive strength decreased with repeated heating cycling, particularly at 500 °C, indicating microstructural damage and weakening of interparticle bonding. Overall, the findings show that cyclic heating, rather than single high temperature event or exposure, drives long-term soil degradation. This shows the importance of considering both thermal history and mineral composition when evaluating lateritic soils for engineering use, particularly in areas exposed to bush burning, wildfires, or thermal remediation.

Supplementary Information The online version contains supplementary material available at https://doi.org/10.1007/s41062-026-02564-7.

Funding This work did not receive grant from any funding agency.

Declarations

Conflict of interest There are no conflicts of interests with regard to this manuscript.

References

1. Azhar M, Mondal S, Tang AM, Singh AK (2024) Effect of temperature on the mechanical properties of fine-grained soils—a review. Geothermics 116:102863. https://doi.org/10.1016/j.geothermics.2023.102863
2. Guo Y, Golchin A, Hicks MA et al (2023) Experimental investigation of soil–structure interface behaviour under monotonic and cyclic thermal loading. Acta Geotech 18:3585–3608. https://doi.org/10.1007/s11440-022-01781-5
3. Liu H, Li J, Zhao M et al (2019) Remediation of oil-based drill cuttings using low-temperature thermal desorption: performance and kinetics modeling. Chemosphere 235:1081–1088. https://doi.org/10.1016/j.chemosphere.2019.07.047
4. Mao W, Ma B, Xu J (2024) Phase change material coated geotextile for temperature regulation of subgrade soil. J Energy Storage 81:110438. https://doi.org/10.1016/j.est.2024.110438
5. Rotta Loria AF, Coulibaly JB (2021) Thermally induced deformation of soils: a critical overview of phenomena, challenges and opportunities. Geomech Energy Environ 25:100193. https://doi.org/10.1016/j.gete.2020.100193
6. Yang W, Sun T, Zhang C, Wang F (2023) Experimental and numerical investigations of thermo-mechanical behaviour of energy pile under cyclic temperature loads. Energy 267:126516. https://doi.org/10.1016/j.energy.2022.126516
7. Alva G, Lin Y, Fang G (2018) An overview of thermal energy storage systems. Energy 144:341–378. https://doi.org/10.1016/j.energy.2017.12.037
8. McCartney JS, Jafari NH, Hueckel T et al (2019) Emerging Thermal Issues in Geotechnical Engineering. In: Lu N, Mitchell JK (eds) Geotechnical Fundamentals for Addressing New World Challenges. Springer International Publishing, Cham, pp 275–317
9. Peduto D, Iervolino L, Foresta V (2022) Experimental Analysis of the Fire-Induced Effects on the Physical, Mechanical, and Hydraulic Properties of Sloping Pyroclastic Soils. Geosciences 12:198. https://doi.org/10.3390/geosciences12050198
10. Sittidumrong J, Jotisankasa A, Chantawarangul K (2019) Effect of thermal cycles on volumetric behaviour of Bangkok sand. Geomech Energy Environ 20:100127. https://doi.org/10.1016/j.gete.2019.100127
11. Bai J, Wang C, Zhang M, Diao Y (2025) A review on drainage of dredged marine soils: Advances and prospects. Mar Georesources Geotechnology 43:260–270. https://doi.org/10.1080/1064119X.2024.2327079
12. Chen Z-J, Feng W, Li A et al (2023) Experimental and molecular dynamics studies on the consolidation of Hong Kong marine deposits under heating and vacuum preloading. Acta Geotech 18:2569–2583. https://doi.org/10.1007/s11440-022-01735-x
13. Ding D, Song X, Wei C, LaChance J (2019) A review on the sustainability of thermal treatment for contaminated soils. Environ Pollut 253:449–463. https://doi.org/10.1016/j.envpol.2019.06.118
14. Sierra MJ, Millán R, López FA et al (2016) Sustainable remediation of mercury contaminated soils by thermal desorption.

Environ Sci Pollut Res 23:4898–4907. https://doi.org/10.1007/s11356-015-5688-8
15. Zihms SG, Switzer C, Irvine J, Karstunen M (2013) Effects of high temperature processes on physical properties of silica sand. Eng Geol 164:139–145. https://doi.org/10.1016/j.enggeo.2013.06.004
16. Baker RS, LaChance J, Heron G (2006) In-pile thermal desorption of PAHs, PCBs and dioxins/furans in soil and sediment. Land Contam Reclam 14:620–624. https://doi.org/10.2462/09670513.731
17. Heron G, Parker K, Galligan J, Holmes TC (2009) Thermal treatment of eight CVOC source zones to near nondetect concentrations. Groundw Monit Remediation 29:56–65. https://doi.org/10.1111/j.1745-6592.2009.01247.x
18. Huon G, Simpson T, Holzer F et al (2012) Situ radio-frequency heating for soil remediation at a former service station: case study and general aspects. Chem Eng Technol 35:1534–1544. https://doi.org/10.1002/ceat.201200027
19. Kingston JLT, Johnson PC, Kueper BH, Mumford KG (2014) In Situ Thermal Treatment of Chlorinated Solvent Source Zones. In: Kueper BH, Stroo HF, Vogel CM, Ward CH (eds) Chlorinated Solvent Source Zone Remediation. Springer, New York, NY, pp 509–557
20. Parker JC, Kim U, Fortune A et al (2017) Data analysis and modeling to optimize thermal treatment cost and performance. Groundw Monit Remediation 37:51–66. https://doi.org/10.1111/gwmr.12199
21. Grant GP, Major D, Scholes GC et al (2016) Smoldering combustion (STAR) for the treatment of contaminated soils: examining limitations and defining success. Remediation J 26:27–51. https://doi.org/10.1002/rem.21468
22. Scholes GC, Gerhard JI, Grant GP et al (2015) Smoldering remediation of coal-tar-contaminated soil: pilot field tests of STAR. Environ Sci Technol 49:14334–14342. https://doi.org/10.1021/acs.est.5b03177
23. Vidonish JE, Zygourakis K, Masiello CA et al (2016) Thermal treatment of hydrocarbon-impacted soils: a review of technology innovation for sustainable remediation. Engineering 2:426–437. https://doi.org/10.1016/J.ENG.2016.04.005
24. Goforth BR, Graham RC, Hubbert KR et al (2005) Spatial distribution and properties of ash and thermally altered soils after high-severity forest fire, Southern California. Int J Wildland Fire 14:343–354
25. Lim MW, Lau EV, Poh PE (2016) A comprehensive guide of remediation technologies for oil contaminated soil—present works and future directions. Mar Pollut Bull 109:14–45. https://doi.org/10.1016/j.marpolbul.2016.04.023
26. O'Brien PL, DeSutter TM, Casey FXM et al (2018) Thermal remediation alters soil properties—a review. J Environ Manage 206:826–835. https://doi.org/10.1016/j.jenvman.2017.11.052
27. Halofsky JE, Peterson DL, Harvey BJ (2020) Changing wildfire, changing forests: the effects of climate change on fire regimes and vegetation in the Pacific Northwest, USA. Fire Ecol 16:4. https://doi.org/10.1186/s42408-019-0062-8
28. Hansen J, Ruedy R, Sato M, Lo K (2010) Global Surface Temperature Change. Rev Geophys 48. https://doi.org/10.1029/2010RG000345
29. Karl DM, Beversdorf L, Björkman KM et al (2008) Aerobic production of methane in the sea. Nat Geosci 1:473–478. https://doi.org/10.1038/ngeo234
30. Certini G (2005) Effects of fire on properties of forest soils: a review. Oecologia 143:1–10. https://doi.org/10.1007/s00442-004-1788-8
31. Mataix-Solera J, Doerr SH (2004) Hydrophobicity and aggregate stability in calcareous topsoils from fire-affected pine forests in southeastern Spain. Geoderma 118:77–88. https://doi.org/10.1016/S0016-7061(03)00185-X
32. Rein G, Cleaver N, Ashton C et al (2008) The severity of smouldering peat fires and damage to the forest soil. CATENA 74:304–309. https://doi.org/10.1016/j.catena.2008.05.008
33. Cekerevac C, Laloui L (2004) Experimental study of thermal effects on the mechanical behaviour of a clay. Int J Numer Anal Meth Geomech 28:209–228. https://doi.org/10.1002/nag.332
34. Geng J, Sun Q (2018) Effects of high temperature treatment on physical-thermal properties of clay. Thermochimica acta 666:148–155. https://doi.org/10.1016/j.tca.2018.06.018
35. Joshaghani M, Ghasemi-Fare O, Ghavami M (2018) Experimental Investigation on the Effects of Temperature on Physical Properties of Sandy Soils. 675–685. https://doi.org/10.1061/9780784481578.064
36. Ma F, Zhang Q, Xu D et al (2014) Mercury removal from contaminated soil by thermal treatment with FeCl3 at reduced temperature. Chemosphere 117:388–393. https://doi.org/10.1016/j.chemosphere.2014.08.012
37. O'Brien PL, DeSutter TM, Casey FXM et al (2016) Implications of using thermal desorption to remediate contaminated agricultural soil: physical characteristics and hydraulic processes. J Env Qual 45:1430–1436. https://doi.org/10.2134/jeq2015.12.0607
38. Roh Y, Edwards NT, Lee SY et al (2000) Thermal-treated soil for mercury removal: soil and phytotoxicity tests. J Environ Qual 29:415–424. https://doi.org/10.2134/jeq2000.00472425002900020007x
39. Afolagboye LO, Arije ZO, Talabi AO, Owoyemi OO (2023) Effects of pre-test heating temperature on microstructure, chemical and mineralogy of lateritic soil. Phys Chem Earth Parts A/B/C 132:103504. https://doi.org/10.1016/j.pce.2023.103504
40. Attah IC, Etim RK (2020) Experimental investigation on the effects of elevated temperature on geotechnical behaviour of tropical residual soils. SN Appl Sci 2:370. https://doi.org/10.1007/s42452-020-2149-x
41. Afolagboye LO, Arije ZO, Talabi AO, Owoyemi OO (2023) Effect of pre-test drying temperature on the properties of lateritic soils. J Nigerian Soc Phys Sci 1109–1109. https://doi.org/10.46481/jnsps.2023.1109
42. Owoyemi OO, Afolagboye LO (2020) Effect of cyclic heating on some engineering characteristics of some soils from Ilorin, Nigeria. https://doi.org/10.1007/s42452-020-03765-0. SN Applied Sciences 2:
43. British Standard 1377 (1990) Methods of test for soils for civil engineering purposes. British Standards Institution, London
44. ASTM D422-63 (2007) Standard Test Method for Particle-Size Analysis of Soils. ASTM International, West Conshohocken
45. ASTM D2166-06 (2016) Standard Test Method for Unconfined Compressive Strength of Cohesive Soil. ASTM International, West Conshohocken
46. Craig RF (2004) Craig's Soil Mechanics, 7th edn. CRC, London
47. Owoyemi OO, Adeyemi GO (2019) Characterisation of soils derived from different parent rocks from north central Nigeria. Proceedings of the Institution of Civil Engineers - Construction Materials 1–14. https://doi.org/10.1680/jcoma.18.00027
48. Becattini V, Motmans T, Zappone A et al (2017) Experimental investigation of the thermal and mechanical stability of rocks for high-temperature thermal-energy storage. Appl Energy 203:373–389. https://doi.org/10.1016/j.apenergy.2017.06.025
49. Fredrich JT, Wong T (1986) Micromechanics of thermally induced cracking in three crustal rocks. J Geophys Research: Solid Earth 91:12743–12764. https://doi.org/10.1029/JB091iB12p12743
50. Basha EA, Hashim R, Mahmud HB, Muntohar AS (2005) Stabilization of residual soil with rice husk ash and cement. Constr

Build Mater 19:448–453. https://doi.org/10.1016/j.conbuildmat.2004.08.001
51. Fredlund DG, Xing A (1994) Equations for the soil-water characteristic curve. Can Geotech J 31:521–532. https://doi.org/10.1139/t94-061
52. Romero E, Vaunat J (2000) Retention curves of deformable clays. Experimental Evidence and Theoretical Approaches in Unsaturated Soils. CRC
53. Lu N, Likos WJ (2004) Unsaturated Soil Mechanics. Wiley
54. Tarantino A (2009) A water retention model for deformable soils. Geotechnique 59:751–762. https://doi.org/10.1680/geot.7.00118
55. Owoyemi O, Afolagboye L (2021) Mineralogy and collapse behaviour of compacted lateritic soils from Northcentral Nigeria
56. Pells P, Robertson A, Jennings JE, Knight K (1975) A guide to construction on or with materials exhibiting additional settlement due to. Collapse of grain structure
57. Liu W, Huang X, Chen Z, Wu J (2025) Resilient and accumulative deformation properties of lateritic soil considering interparticle cementation damage. Eng Geol 356:108304. https://doi.org/10.1016/j.enggeo.2025.108304
58. Opukumo AW, Davie CT, Glendinning S, Oborie E (2022) A review of the identification methods and types of collapsible soils. J Eng Appl Sci 69:17. https://doi.org/10.1186/s44147-021-00064-2
59. Hemanth P, Krishnaiah S (2025) Thermo Mechanical and Microstructural Behavior of Clay Soil Under Elevated Temperatures with CBR Prediction Modelling. IJSER 15–22. https://doi.org/10.70729/SE251214171541
60. Pan T, Zhao Z, Ma J, Liu F (2025) Experimental investigation of mechanical properties and pore characteristics of Hipparion Laterite under freeze–thaw cycles. Appl Sci 15:5202. https://doi.org/10.3390/app15095202
61. Pandya S, Sachan A (2020) Variation of collapse potential and stiffness degradation with matric suction of compacted unsaturated cohesive soil. Int J Geotech Eng 14:35–48. https://doi.org/10.1080/19386362.2017.1398368
62. Afolagboye LO, Owoyemi OO, Abdu–Raheem YA, Adeoye AS (2024) Effects of elevated temperature and treatment duration on selected index and engineering properties of lateritic soils. Discov Civ Eng 1:71. https://doi.org/10.1007/s44290-024-00077-9
63. Somerton WH (1992) Thermal properties and temperature-related behavior of rock/fluid systems. Elsevier, Amsterdam
64. Frost RL, Horváth E, Makó É et al (2003) Slow transformation of mechanically dehydroxylated kaolinite to kaolinite—an aged mechanochemically activated formamide-intercalated kaolinite study. Thermochimica acta 408:103–113. https://doi.org/10.1016/S0040-6031(03)00316-2

Publisher's note Springer Nature remains neutral with regard to jurisdictional claims in published maps and institutional affiliations.

Springer Nature or its licensor (e.g. a society or other partner) holds exclusive rights to this article under a publishing agreement with the author(s) or other rightsholder(s); author self-archiving of the accepted manuscript version of this article is solely governed by the terms of such publishing agreement and applicable law.